



ORIGINAL RESEARCH ARTICLE

Friction and Wear Behavior of Al-Graphene Nanocomposite Synthesized by Powder Metallurgy and Hot Extrusion

M.R. Haseebuddin, R. Keshavamurthy, and S.J. Niteesh Kumar

Submitted: 27 June 2023 / Revised: 28 August 2023 / Accepted: 8 September 2023

In this research work, Al matrix is reinforced with graphene, synthesized by the powder metallurgy method, and further processed by the hot extrusion process. The microstructure of aluminum and Al-graphene composite samples was investigated using FESEM and optical microscopy. The grain structure is investigated to analyze the grain size of pure aluminum and aluminum-graphene composites. Pin on Disk wear test setup is used to investigate the tribological behavior of the developed composites. Developed samples were tested experimentally to evaluate the influence of graphene addition, applied load, and sliding velocity on wear behavior. From the results, the wear rate of Al-Graphene composites is observed to be lower compared to monolithic aluminum samples. However, wear rate increases with the increase in velocity of sliding and the applied load. The Coefficient of Friction (COF) of composite samples was less than that of pure aluminum samples. Results reveal that the graphene-Al composites exhibit superior tribological properties during tribological tests and exhibit a 38.1% reduction in wear rate at a 60 N load.

Keywords composite, extrusion, friction, graphene, powder metallurgy, wear

1. Introduction

Aluminum has diverse range of applications, including aerospace sector, automotive industry, and in the production of military hardware. In addition, alloys of aluminum that have superior mechanical and physical properties (Ref 1-6), such as a low specific weight and thermal expansion coefficient, a high specific modulus, and a high specific strength, the addition of particulate reinforcement will help to resist wear by minimizing the amount of micro-cutting that occurs and by forming a protecting layer of oxide between composite surfaces (Ref 7).

Aluminum and the alloys made from it do not have a very good resistance to wear, and there are many different ways that the tribological behavior of aluminum alloys could be enhanced. Wear and friction can be minimized by the use of lubricants; however, in all service conditions, it is not practical to use any lubricants or grease. Furthermore, it has been observed that under lubricated conditions, a protective layer can form on the surface of the composite (Ref 10). Techniques such as PVD, CVD, plasma spraying and friction surfacing can be used to intentionally create such a protective lubricant layer (Ref 5-10). These methods enable the application of coatings to the surface of the material, facilitating the formation of a

protective layer that can improve its performance under lubricated conditions. Through the application of coatings in conjunction with micro-texturing, researchers have been successful in improving both the levels of performance and the strength of materials in conditions that require high tribological performance. Now that advanced coatings can be produced, applications that require a high level of tribological resistance can find coatings that meet their high performance and durability requirements (Ref 10). These coatings have their own drawbacks, such as poor adhesion, oxidation, and degradation over time, which are all caused by time. Incorporating carbonous reinforcements in the matrix materials can help solve the issues that arise from the use of liquid lubricants, grease lubricants, and coatings (Ref 11, 12).

Reinforcement of Al with graphite, graphene and MWCNT, which are carbon-based materials, can improve the tribological, mechanical, and electrical properties of MMCs (Ref 13). In many applications SiC is used as reinforcement material; however, Al₂O₃ (Ref 14), graphite, and various nanoparticles have also been used as reinforcements. Furthermore, carbon nanotubes (CNT) and graphene have been used in a variety of applications, including as lubricant additives and reinforcing agents in ceramic matrix composites (Ref 15-17). Incorporation of nanoscale SiC particles to develop Al-SiC nanocomposites significantly increases the hardness of materials, and it is observed that there is reduction in dry sliding wear as well as corrosive wear. Reinforcement of Al with nanosilicon carbide significantly increases the hardness of materials, reduces the amount of wear due to dry sliding, and has shown a reduction in corrosive wear. Al/SiC nanocomposites, when compared with base alloys, have significantly improved overall strength as well as their resistance to corrosion and wear (Ref 18). The incorporation of nanocarbonous particles into polymer-based composites has shown improvement in the tribological properties of the materials (Ref 19-21). It has been demonstrated

M.R. Haseebuddin, R. Keshavamurthy, and S.J. Niteesh Kumar, Department of Mechanical Engineering, Dayananda Sagar College of Engineering, Bangalore 560111, India. Contact e-mail: haseebdsce@gmail.com.

that the combination of reinforcement of SiC(n) and MWCNT with Al significantly reduces the composite wear rate (Ref 22, 23). It has been observed from the literature that when the sliding speed or load increases, the wear shifts from mild to severe and the lubricating coating is irreparably damaged (Ref 24). In graphene-reinforced aluminum composites, there are fewer craters, exfoliation, and scratches, according to research (Ref 25, 26).

Graphene possesses excellent mechanical and tribological properties, which have attracted attention of many. Scientists have researched graphene in recent years and recommend it as a remarkable reinforcement candidate for multi-material composites (MMCs), ceramics, and polymer-based composites. Graphene is composed of carbon atoms, it is also defined as a thick sheet made of carbon. Because of its low density and exceptional physical properties, graphene's original structure is the arrangement of carbon atoms as a sheet. Graphene has the potential to be used as a reinforcement in high-strength applications because of these characteristics. Numerous studies have demonstrated that individual nanosheets of graphene possess very high mechanical, thermal, and electrical properties. Because graphene has a high tensile strength and is a good thermal conductor, it is preferred in the manufacture of battery cells, heat sinks, and printed circuit boards (Ref 8-13, 27-29).

Composite samples were fabricated through a two-step process involving ball milling and selective laser melting (SLM). Various compositions were tested, containing 0.5%, 1.0%, and 2.5% by weight of graphene. Interestingly, the composite with 2.5% graphene exhibited issues with agglomeration, which negatively impacted its mechanical properties (Ref 30).

Furthermore, it is worth noting that in certain instances, the addition of graphene to the aluminum has led to an enhancement in strength. However, beyond a critical percentage of graphene, the material's properties deteriorated (Ref 31, 32). This suggests that there's a delicate balance in the composition of al-graphene composites, where adding graphene can enhance strength up to a certain point, but an excessive amount may have adverse effects on the material's performance. These findings underscore the importance of optimizing the graphene content for specific applications to achieve the desired mechanical properties.

Numerous researchers have utilized solid-state processing methods in order to synthesize metal matrix nanocomposites with graphene reinforcement (Ref 33, 34). Mechanical properties of MMC's can be improved by reinforcing the matrix by the following materials: Graphene has been used as a reinforcement material in magnesium (Ref 35), copper (Ref 36), and aluminum (Ref 37-41). On the other hand, there is limited data available on wear behavior of MMC's with graphene as a reinforcement. Hence, an attempt has been made to develop graphene-reinforced aluminum composites and experimentally evaluate the tribological behavior of the newly developed Al-Graphene composite.

2. Experimentation

Pure aluminum in the form of powder is the matrix material used for the development of composite samples. Aluminum powder has 98% purity, particle sizes in the range of 20-45

microns, and a density of 2.71 g/cc. Another material used is graphene nanoparticles of purity 99%, particle size 5-10 microns, and density 0.24 g/cc. Figure 1(a) and (b) shows the SEM pictures of aluminum and graphene powders, respectively. Pure aluminum samples and an Al-graphene composite sample with 1% by weight graphene content were developed using the stir casting method.

2.1 Magnetic Stirring

Magnetic stirring is used to mix graphene particles in aluminum matrices. Aluminum-graphene MMCs are mixed with a magnetic stirrer after being dispersed in 99 percent pure ethanol. The stirring speed is set to 700 rpm, and the mixture is continuously stirred for one hour, as shown in Fig. 2. The stirring has stopped, and the al-graphene slurry has been allowed to settle completely. The excess ethanol present in the solution is filtered using a filter paper. Then heating furnace is used to dry the powder for approximately 6 h at a temperature of 500 °C.

2.2 Blending of Composites

Universal mini ball milling set up is as shown in Fig. 3(a). Graphene dispersed homogeneously in Al matrix will have an influential effect on the performance of composite, hence the dried powders are blended using a mini ball mill. The powders are ball milled using a Universal mini ball mill with a ball-to-powder ratio of 5:1. A constant speed of 300 rpm is maintained and each sample is mixed for 2 hours. The powder samples are loaded into chamber and sealed properly. As shown in Fig. 3(b), each ball is having a weight of 33.708 g and 10 balls are used for ball milling at a speed of 300 rpm for milling the composite powders. The steel balls in the vessel will collide due to the rotary action of the vessel and also the balls will collide with the container. These collisions cause cold welding of graphene with Al particles. These collisions take place for two hours in the ball milling chamber causing homogeneous dispersion of graphene.

2.3 Powder Compaction and Sintering

Graphene-Al composite samples are prepared by using ball milled powder and further compacting. Compaction of powder is done by using a single acting uniaxial hydraulic press of 100 ton load capacity (Fig. 4b). Copper shells of inner diameter 24.5 mm, 26.5 mm outside diameter and having a height of 35 mm are prepared with the purpose of avoiding the damage to die. It is shown in Fig. 4(a) ball milled powder is filled in copper shell.

After compaction, the graphene-alcohol samples are sintered for 4 h in a furnace at around 585 °C (Fig. 4c). After appropriate sintering, the copper shell surrounding the composite samples is removed, the sintered samples are hot extruded, and the secondary processing operation is completed. The samples are hot extruded at a temperature of 400 °C. The prepared composite samples are cut, and test specimens are prepared in accordance with ASTM G99-05 standards before being tested. Scanning electron microscopy, optical microstructure, and grain size analysis were performed on the test samples. Pin on Disk Wear tests are performed on the developed composite samples at various loads and sliding distances.

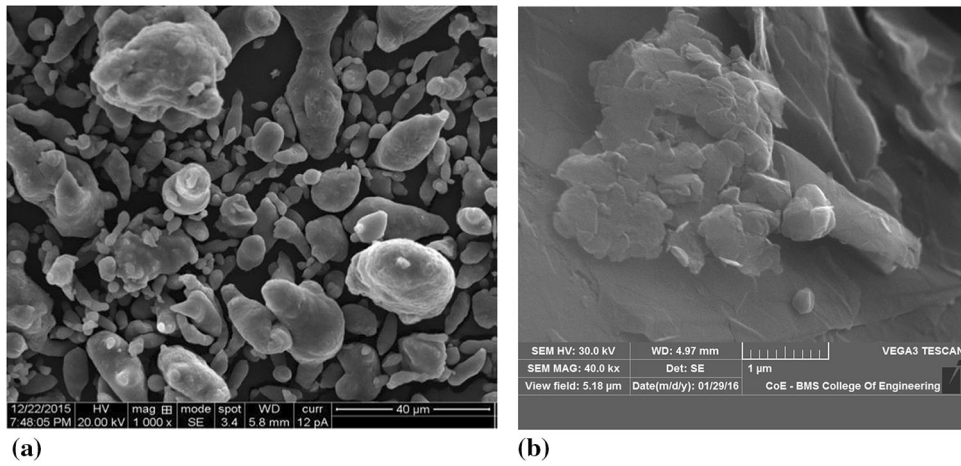


Fig. 1 (a) SEM of Aluminum powder. (b) SEM of Graphene Nanosheets

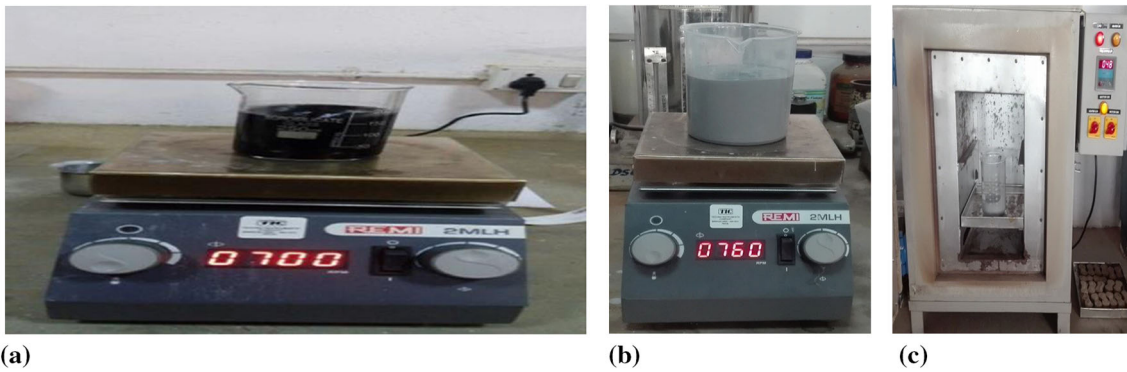


Fig. 2 Dispersion of powders using Magnetic stirring setup (a) Dispersion of Graphene. (b) Dispersion of Al-Graphene. (c) Powder kept in Heating furnace

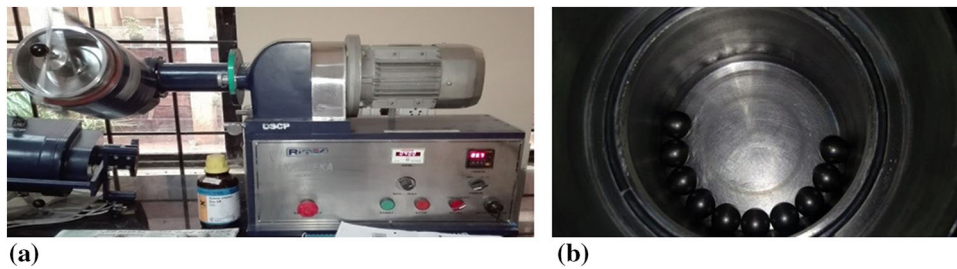


Fig. 3 Photograph of (a) Universal mini ball mill. (b) Balls inside vessel

2.4 Friction and Wear Test

The wear test to determine the wear behavior of developed aluminum and Al-graphene composites was conducted using a pin-on-disk experimental test set up as shown in Fig. 5(a). Test specimens of size 8 mm in diameter and height 25 mm were prepared in accordance with ASTM G99-05 from compacted samples for conducting the test (Ref 42). A lap grinding machine is used to polish the cut specimen before conducting the experimental tests. Tests were carried out on different specimens with varying loads at 20, 40, and 60 N. Also, the sliding velocities are varied, and tests are repeated at velocities of 0.25, 0.5, and 0.75 m/s, whereas the test time period is kept

constant at 20 minutes. The test specimen, also called a pin, is pressed against the rotating disk (en31-steel) by applying the load in the pan. The test setup is equipped with an arm for detecting friction, and it also holds the specimen vertically on a rotating disk with the application of a load. The frictional traction force is measured using a PC-based data logging system. The results appear on the screen, and the results are documented for post-test analysis. The wear behavior and friction of the prepared composites were studied at various loads and sliding velocities. Each test of tests are repeated three times, and the graphs are plotted using the average values of the results obtained.

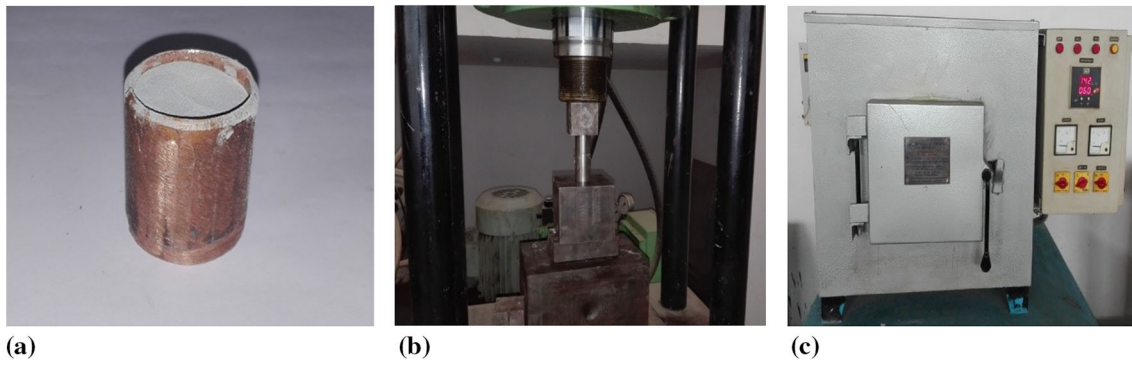


Fig. 4 Photographs of (a) Powder filled into copper shells. (b) Punch and die along with samples loaded on Hydraulic press. (c) Sintering furnace

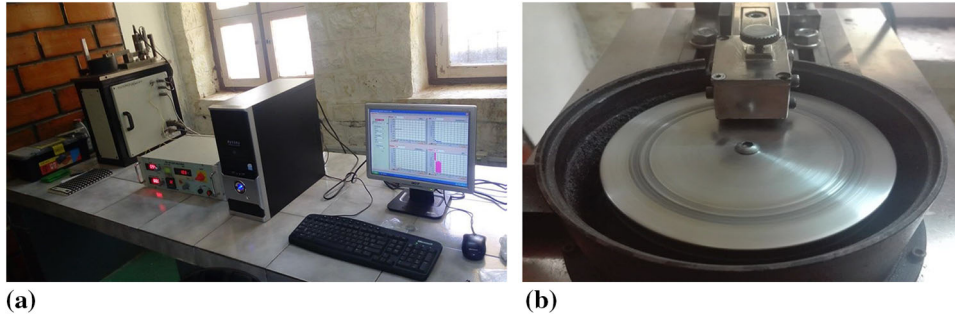


Fig. 5 Photographs of (a) Wear testing setup (Pin on disk setup). (b) Sample under testing

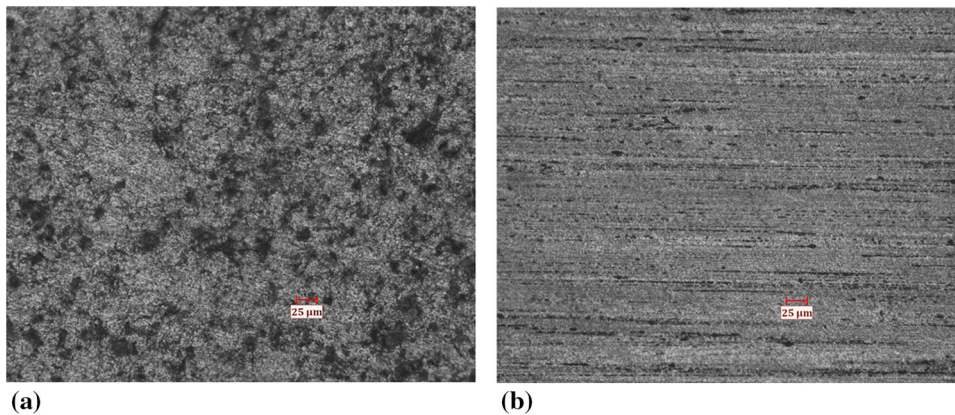


Fig. 6 Optical micrographs of (a) Pure Al Sample. (b) Al-Graphene composite

3. Results and Discussion

3.1 Microstructure

Optical micrographs of a pure aluminum sample that has undergone hot extrusion are shown in Fig. 6(a), while Fig. 6(b) presents the optical micrographs of graphene-reinforced aluminum composite sample. The optical micrographs were obtained in a manner aligned with the extrusion process. Upon observing these micrographs, it becomes evident that the composite material exhibits a notable and uniform distribution of fine graphene particles. One noteworthy characteristic is the

alignment of graphene particles in accordance with the direction of material flow, which is achieved through the extrusion procedure.

Upon conducting a more detailed analysis at increased levels of magnification, it becomes apparent that a robust and clearly defined bond is present between the matrix, which in this case is aluminum, and the reinforcement material, which is graphene. The strong bonding observed can be ascribed to the thermo-mechanical processing employed during the hot extrusion procedure. The manufacturing technique described herein plays a pivotal role in the fragmentation of agglomerated particles, thereby making a substantial contribution to the

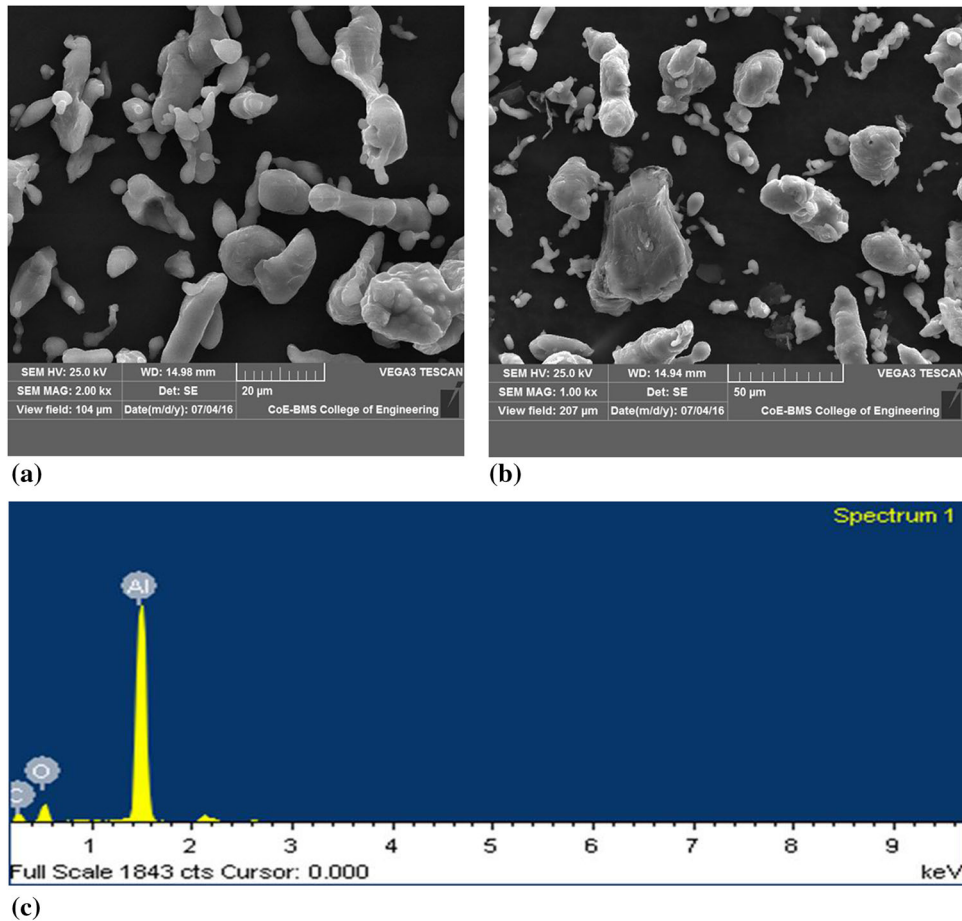


Fig. 7 (a) SEM of ball milled Al powder. (b) SEM of Al-Graphene composite. (c) EDS pattern of composite

reinforcement material's improved bonding with the matrix. The establishment of this bond is crucial for ensuring the comprehensive structural integrity and optimal performance of the composite material composed of graphene-reinforced aluminum.

3.2 Powder Morphology

Figure 7(a) shows the scanning electron microscopy pictures of aluminum powder. SEM pictures of aluminum powder with graphene nanoparticles added are shown in Fig. 7(b). EDAX of the aluminum-graphene composite mixture is presented in Fig. 7(c). In the beginning of low-energy ball milling, adhesion of graphene particles to the surface of aluminum particles takes place due to a phenomenon called cold welding. As the milling time increases, the coagulation will lead to the particles getting bulkier. Also, there will be collisions between Al and graphene particles, balls, and the ball milling vessel's inner surface. The particles become flat due to repeated hammering of the balls, resulting in the composite powder being subjected to crushing. Fine to coarse powder can be observed, with particle sizes ranging from 5 to 40 μm. From the SEM images it is evident that graphene is uniformly distributed in the aluminum matrix.

Figure 8(a) depicts the XRD pattern of a Pure Al sample after sintering. The peaks obtained at angles 38°, 45°, 65°, and 78° can be seen in this image, confirming the presence of Al in the compacted sample. After sintering the XRD pattern of an Al-graphene composite obtained is depicted in Fig. 8(b). Along

with the Al peaks mentioned above, we can see some additional peaks at angles 26°, 29°, 38°, 42°, 57°, 62°, 69°, and 74° in the image. This demonstrates the presence of graphene and aluminum in the composite sample.

FESEM images in Fig. 9 and EDS spectra shown in Fig. 10 confirm homogenous distribution of graphene in aluminum matrix, and it is also clear that the matrix and reinforcement material have good bonding. The ball milling process combined with the hot extrusion process had a significant impact on dispersion and interfacial bonding. Further, EDS mapping confirmed the homogeneous dispersion of the graphene (Fig. 11). From the results obtained, it is evident that graphene is uniformly distributed in the aluminum matrix.

3.3 Grain Size Analysis

The composite specimen is subjected to grain size analysis. The specimen is first polished, then subjected to etching with Keller's etchant and then subjected to grain size analysis. Figure 12(a,b) depicts the result of the pure Al grain size analysis, whereas Fig. 13(a,b) depicts the result of the Al-Graphene composite grain size analysis.

The obtained results show that the composite specimen's grain size is smaller compared to grain size of pure Al, as shown in Table 1. This suggests that grain refining has a strong relationship with the content of reinforcement. Because the grains in composite are finer, it has greater strength than pure alloy. Grain size has been reduced as a result of the mechanism

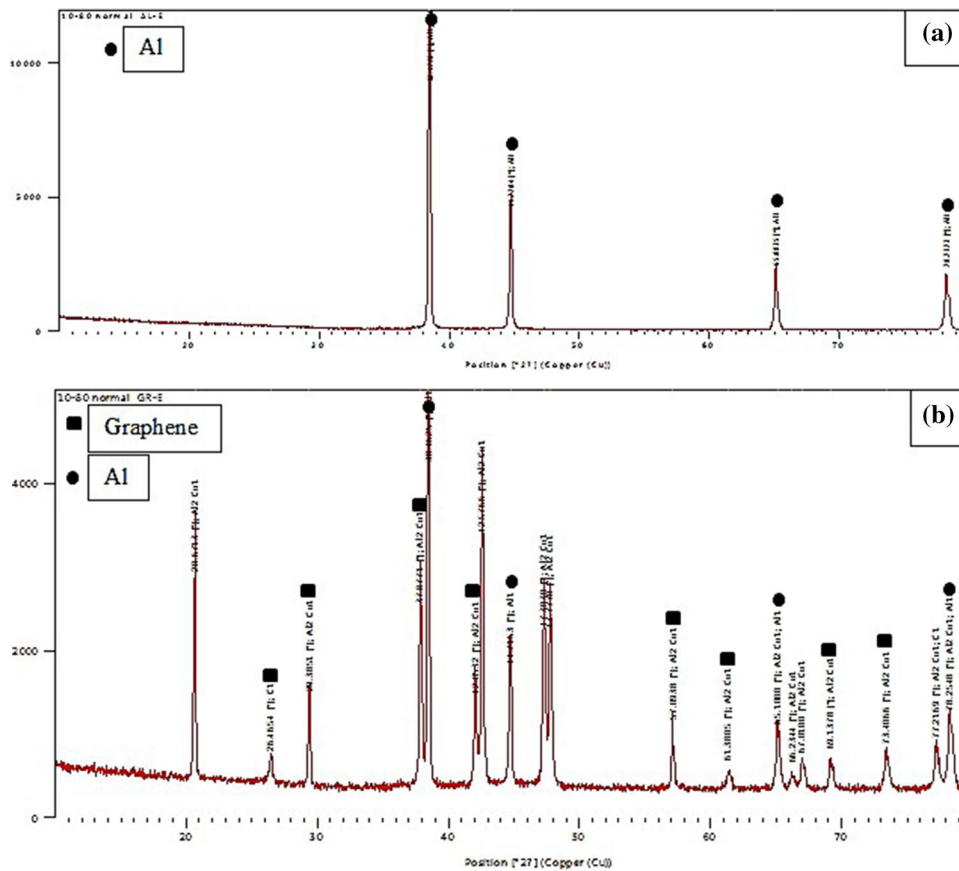


Fig. 8 (a) XRD of Pure Aluminum. (b) XRD of Composite

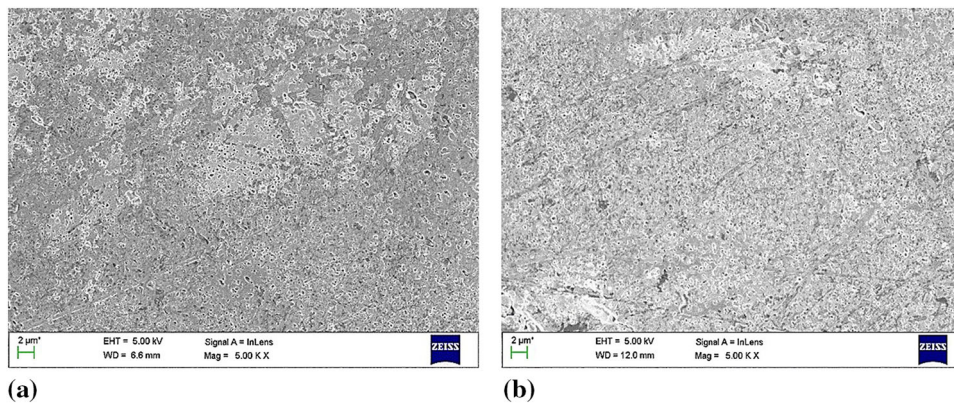


Fig. 9 FESEM micrographs of (a) Pure Aluminum. (b) Aluminum-Graphene composite

known as grain wrapping. Wrapping graphene sheets around grains prevents grain growth resulting in the grain size of the composite sample to be smaller compared to grain size of pure aluminum.

3.4 Friction and Wear Test

3.4.1 Coefficient of Friction (COF). The experimental findings indicate that the frictional coefficient is greater for unreinforced aluminum in comparison to the Al-graphene composite. At a load of 20 N, the COF exhibits a minor value, which subsequently escalates as the load magnitude increases.

Figure 14 illustrates the correlation between the COF and the applied load, while maintaining a constant sliding velocity of 0.25 m/s. The observed pattern aligns with the relationship between load and wear rate.

During the process of sliding, the contact surfaces undergo a tribochemical reaction, resulting in the formation of layers. These layers play a vital part in determining the tribological behavior of the composite sample, particularly under low and medium loads. The hardness and mechanical stability of the formed layers exhibit a decrease when subjected to higher loads, consequently leading to an observed increase in the COF.

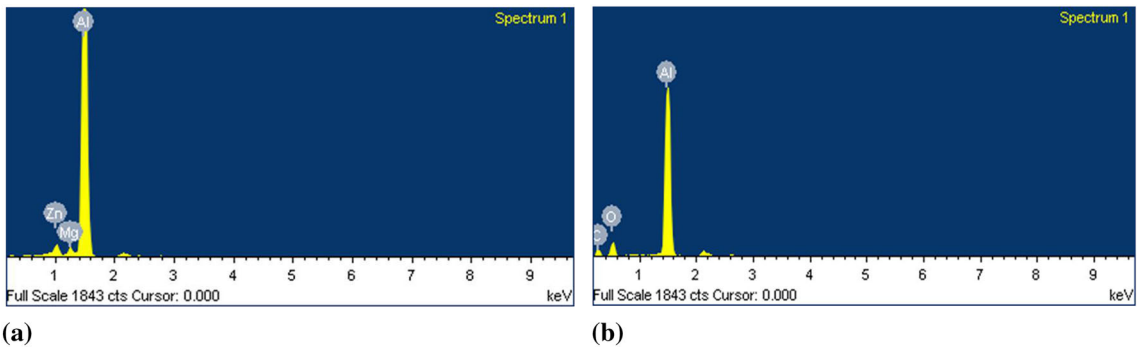


Fig. 10 EDS spectra of (a) Pure Aluminum. (b) Aluminum-Graphene composite

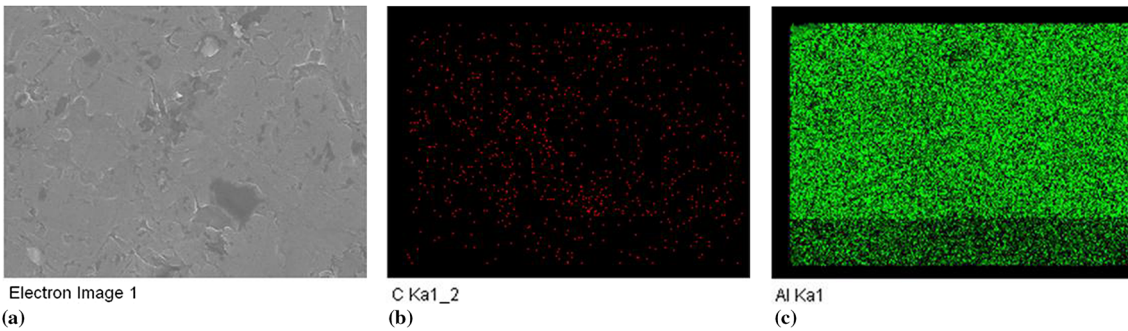


Fig. 11 EDS mapping results of composite

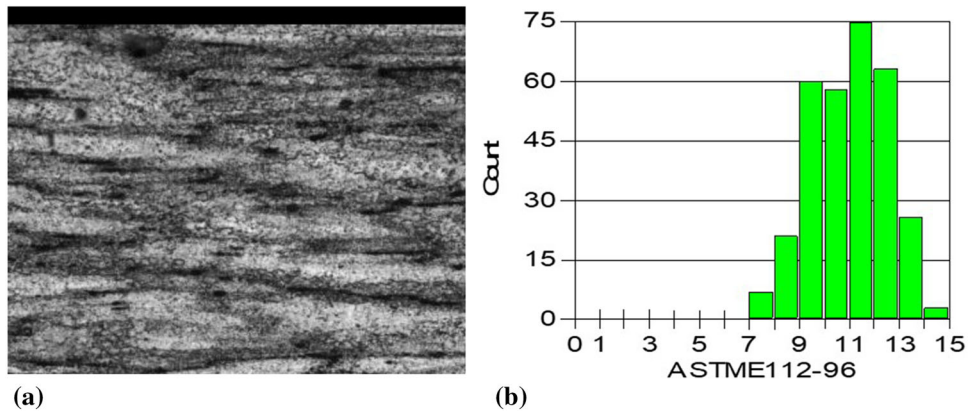


Fig. 12 Pure Al (a) Image at Magnification 200X. (b) Grain count.

Moreover, the coefficient of friction exhibits a strong dependence on reinforcements. Notably, when comparing reinforced composites to unreinforced aluminum, it was observed that the coefficient of friction decreased under higher load conditions.

The incorporation of graphene into aluminum has the potential to significantly reduce the coefficient of friction. Graphene possesses a unique structural composition characterized by a single-layer configuration of carbon atoms, in a hexagonal lattice pattern arrangement. The incorporation of graphene into the aluminum matrix leads to modifications in the surface characteristics, consequently impacting the frictional response exhibited by the composite system. Graphene demonstrates remarkable characteristics when employed as a solid lubricant. The capacity for sliding motion in graphene sheets is readily observed, a characteristic that can be attributed to their inherent two-dimensional structure (Ref 43-45). The utilization

of graphene as a coating on aluminum surfaces can function as a lubricant, thereby reducing the occurrence of direct contact between the individual metal surfaces. The phenomenon of reduced friction is observed when graphene sheets slide between the surfaces of aluminum. Graphene exhibits a highly homogeneous atomic structure, which is distinguished by a monolayer configuration of carbon atoms. The integration of aluminum and graphene yields a more polished surface in contrast to the unadorned metallic counterpart. The relationship between the decrease in surface roughness and the likelihood of asperities, which are minor surface irregularities, coming into contact is inversely proportional. This relationship has a significant impact on the occurrence of friction. Graphene demonstrates exceptional resistance to wear. Upon being introduced into the aluminum matrix, it initiates the formation of a protective layer that demonstrates resistance to wear and

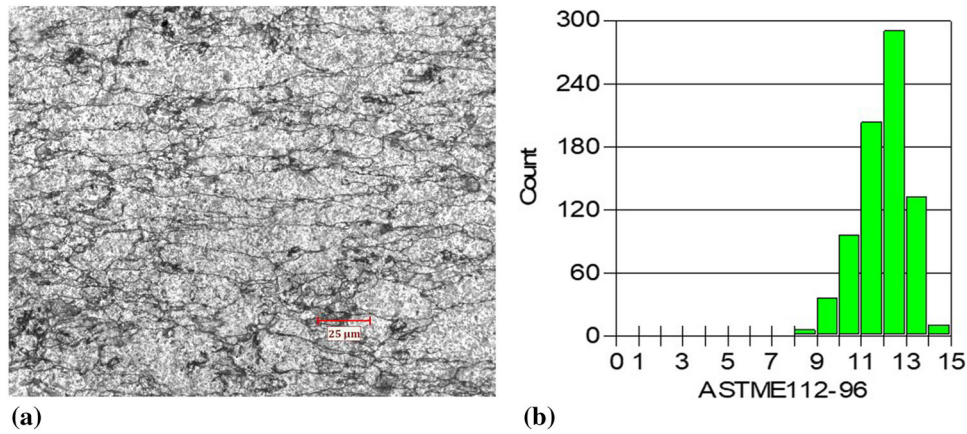


Fig. 13 Composite (a) Image at magnification 500X. (b) Grain count

Table 1 Results of grain size analysis

Specimen	Grain count	Min. grain size	Max. grain size	Avg. grain size no.	Average Grain Size, μm
Pure Al	428	7.44	14.62	7.16	29.3
Composite	778	7.46	14.44	7.46	23.8

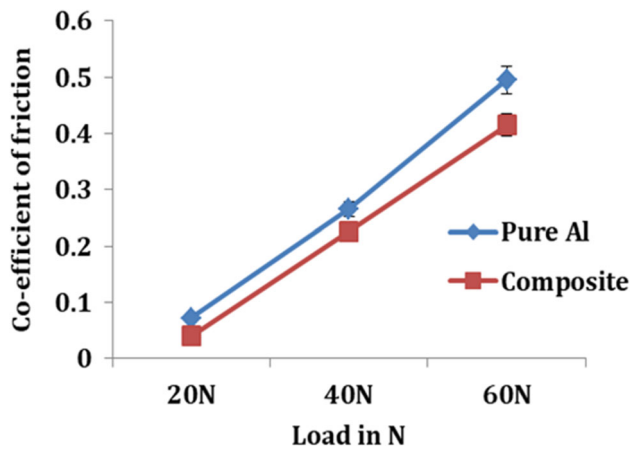


Fig. 14 Variations in Coefficient of Friction with respect to Load.

simultaneously reduces the production of wear debris. Hence there is a reduction in the component of friction (Ref 46, 47).

Figure 15 depicts the relationship between the sliding velocities and COF for both unreinforced aluminum and its composite material. The coefficient of friction is inversely proportional to sliding velocity, as depicted in Fig. 14. Consequently, the coefficient of friction can be considered a dependent variable that is influenced by the sliding velocity. A consistent load of 20N is maintained during the experimental tests, while the sliding velocity was adjusted within the range of 0.25 to 0.75 m/s. As previously mentioned, all experimental procedures were carried out under ambient conditions. In the event of pure aluminum, an escalation in sliding velocity will lead to the development of an electrochemical layer. Aluminum oxide (Al_2O_3) is formed due to the he reaction between aluminum (Al) and oxygen (O_2). It is well-established that Al_2O_3 possesses exceptional lubrication properties.

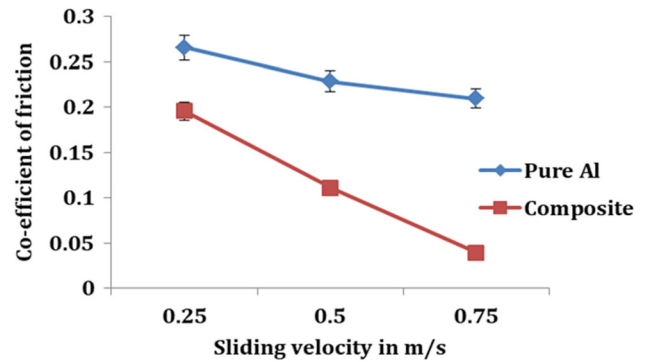


Fig. 15 Variations of Coefficient of friction with respect to sliding velocity

Therefore, it is evident that the coefficient of friction is decreased. The inclusion of graphene, a material renowned for its exceptional lubrication properties, distinguishes the composite sample. The formation of an oxide layer between the sliding surfaces leads to a reduction in the coefficient of friction. The influence of temperature on the coefficient of friction (COF) was recognized as an additional significant factor. Consistent coefficients of friction (COF) values were obtained when tests were conducted under controlled and constant temperature conditions.

Additionally, it has been acknowledged that the surface finish of both the composite material and the counter surface has an impact on the coefficient of friction (COF). The stability of coefficient of friction (COF) measurements was varied when these surfaces were consistently prepared with comparable finishes. Presence of beneficial layers on worn out surfaces has been confirmed by EDA analysis which confirms the rich oxides on the surface.

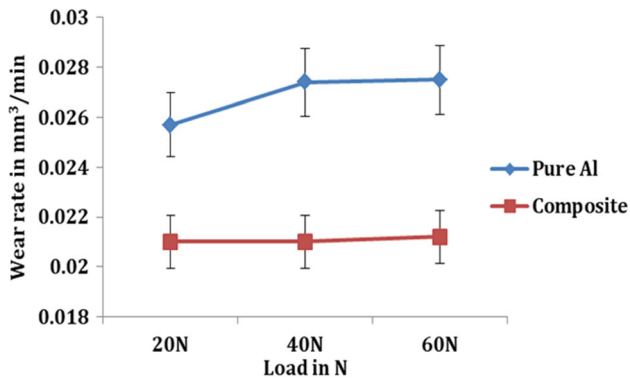


Fig. 16 Wear rate variation with respect to Load

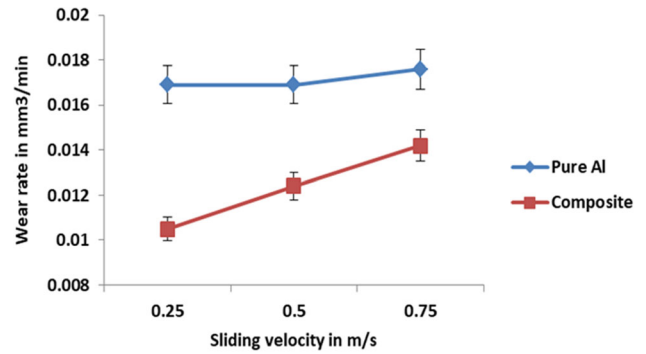


Fig. 17 Wear Rate variation with respect to Sliding Velocity

3.4.2 Wear Rate. The wear rate exhibits variation with changes in load recorded at a constant sliding velocity of 0.25 m/s as depicted in Fig. 16. Based on graph plotted, it is apparent that the wear loss is significantly more in the unreinforced aluminum sample compared to the composite sample. Additionally, it is noteworthy that the composite sample exhibits a considerable reduction in wear loss. At higher loads, unreinforced aluminum exhibits a propensity for significant plastic deformation. As a result wear debris is formed on the surface due to the application of higher loads during plastic deformation which leads to increase in the wear rate. Continued augmentation of plastic deformation will give rise to subsurface cracking, thereby resulting in an elevated level of material removal. The initiation of delamination is observed to coincide with the application of elevated loads, subsequently resulting in an escalation of wear loss. This demonstrates the efficacy of reinforcements in enhancing the performance of an Aluminum matrix. When graphene, a material renowned for its exceptional mechanical characteristics, is distributed throughout its matrix, it serves to enhance the strength and stiffness of aluminum, as documented in reference (Ref 48). Moreover, the incorporation of graphene with aluminum results in the manifestation of solid lubrication properties, primarily attributed to its remarkably low coefficient of friction and unique two-dimensional structure. The aforementioned characteristic of this property serves to diminish the occurrence of friction between surfaces that are in motion relative to each other, thereby resulting in decreased rates of wear and extended lifespan of the components (Ref 49). Graphene has good thermal conductivity which contributes to the enhancement of heat dissipation in aluminum. The enhanced heat dissipation results in a reduction in wear and material degradation by effectively mitigating excessive temperature increases at the interface where wear occurs (Ref 50). Graphene has the ability to form protective layers on aluminum surfaces, effectively these layers act as a practice barrier between the aluminum matrix and the counter surfaces, thereby impeding direct contact between them. The presence of this protective layer serves to mitigate the loss of material that occurs during contact involving sliding or rubbing, thereby reducing the occurrence of abrasive wear (Ref 51).

The effect of sliding velocity on the wear rate of tested samples is observed in Fig. 17. The wear loss of unreinforced aluminum exhibits a higher magnitude when compared to the reinforced samples at varying sliding velocities. The incorporation of weight percentage of Graphene leads to a significant reduction in the wear rate. Therefore, the increased hardness of the composite material is accountable for the observed

enhancement in wear rate. The experimental findings indicate that the wear rate of unreinforced Aluminum samples is higher in comparison to its composite counterpart. Furthermore, it should be noted that an increase in speed leads to a corresponding increase in the wear rate of both unreinforced Aluminum and its composite material. However, the amount of wear experienced by composites is lower in comparison to that of pure alloys.

As previously mentioned, the wear resistance of the composite material has been enhanced as a result of the heightened hardness. The enhanced hardness of the composite material can be attributed to the incorporation of reinforcement within the aluminum matrix. The low sensitivity of wear rate to variations in load during the testing of graphene-reinforced aluminum composites can be attributed to several significant factors. To begin with, when the composite material exhibits elevated levels of hardness and toughness properties, it experiences reduced vulnerability to damage caused by wear. In instances of this nature, the material demonstrates a high capacity to endure mechanical stresses resulting from escalating loads, while simultaneously displaying negligible signs of wear. Moreover, Graphene is widely recognized for its exceptional lubrication characteristics. Graphene demonstrates the capability to function as a solid lubricant, even when subjected to substantial loads, thereby effectively mitigating friction and minimizing wear at the interface between contacting surfaces. The intrinsic characteristic of graphene serves to counterbalance the possible acceleration of wear due to heightened loads, leading to a comparatively uniform rate of wear throughout the range of loads. Furthermore, it is possible that the composite material exhibits an efficient mechanism for distributing loads. The utilization of this mechanism facilitates the dispersion of the applied load in a more even manner over a greater expanse, thereby effectively alleviating concentrated stresses that may lead to deterioration. The incorporation of graphene into the composite material enhances load distribution and enhances the structural integrity of the material. Additionally, it is conceivable that the selected load range for experimentation does not encompass a regime in which there is a substantial alteration in the wear characteristics of the material. Certain materials exhibit a uniform rate of wear within a defined range of loads. However, it is only when subjected to loads exceeding this range that more noticeable deviations in wear characteristics become apparent. The aforementioned phenomenon underscores the importance of meticulously choosing load parameters for testing purposes and acknowledging the inherent wear characteristics of the material within that specific range.

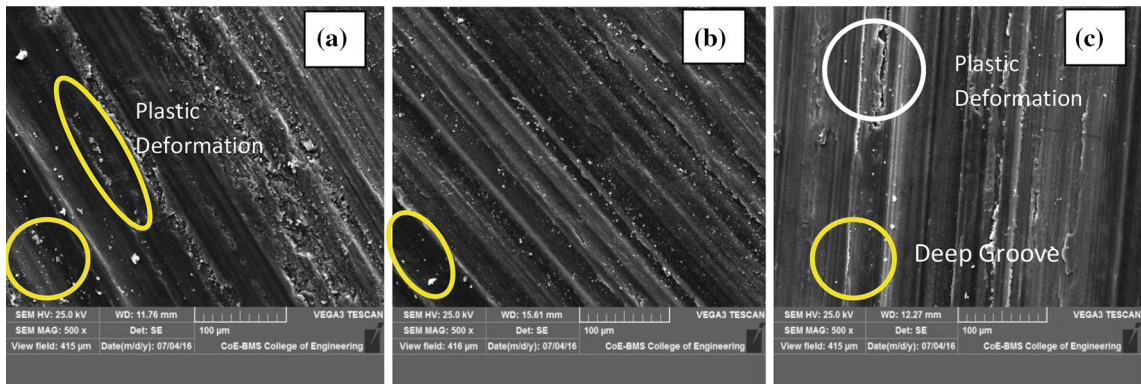


Fig. 18 SEM images of worn surfaces of Pure Al at load (a) 20N. (b) 40N. (c) 60N

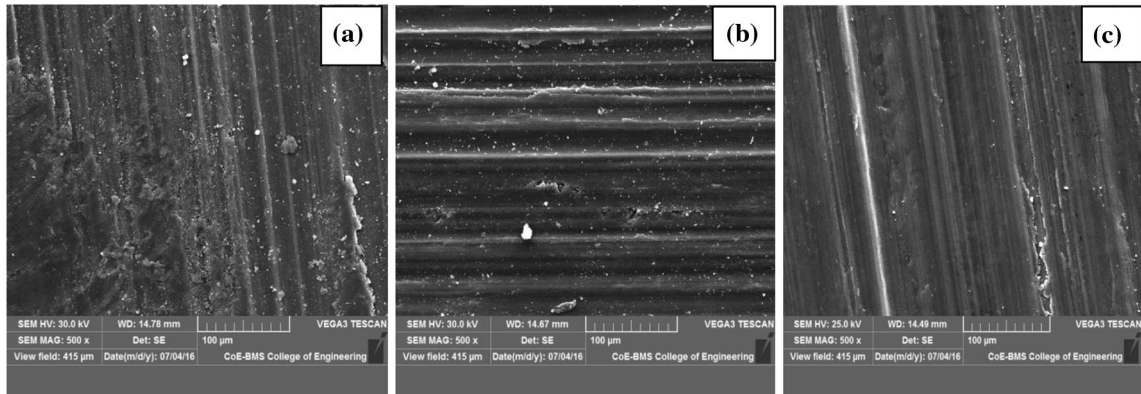


Fig. 19 SEM images of worn surfaces of composite at load (a) 20N. (b) 40N. (c) 60N

3.4.3 Examination of Worn Surface and Wear Debris. Figure 18 depicts Scanning Electron Micrographs (SEMs) of pure aluminum (Al) samples, showcasing the worn surfaces under varying loads, specifically 20, 40, and 60N. Figure 19 displays the scanning electron microscope pictures of worn surfaces of composite samples subjected to various loads, specifically at 20, 40, and 60N, respectively. Figure 18 illustrates a significant extent of plastic deformation, characterized by the formation of deep grooves aligned with the sliding direction. Additionally, the presence of agglomerated debris particles is also discernible in the observation. The resulting debris consists of a combination of Aluminum and EN31 steel, which is the material of the pin. The shallow extent of plastic deformation and penetration of grooves in Al-Graphene composite samples is evident in Fig. 19. The pin-on-disk test results exhibit a strong correlation with the accompanying images, providing evidence of a reduced wear rate in the composite material. The phenomenon of heat generation between the wear surfaces during sliding under the influence of a load leads to the continuous oxidation of the formed debris. The formation of a tribochemical layer between the contacting surfaces serves to provide protection, resulting in a decrease in both the rate of wear and the coefficient of friction. The aforementioned layer is referred to as the mechanically mixed layer, which comprises a combination of aluminum and graphene particles, as previously discussed. At elevated loads,

there is an observed increase in plastic deformation occurring at the interface of the mating surfaces. The augmented dimensions and extent of the grooves in unreinforced composites contribute to the heightened plastic flow. However, it should be noted that in composite samples, no such alterations are observed. The experimental results demonstrate the capacity of a prepared composite material to sustain its mechanical properties under elevated loads during the wear testing procedure.

The debris obtained following the completion of wear test was analyzed using scanning electron microscopy and energy-dispersive x-ray spectroscopy (EDS), as depicted in Fig. 20(a) and (b), respectively. The SEM image presented in Fig. 20(a) depicts Pure Al wear debris at a magnification of 500X. The SEM micrographs at 500X magnification and EDS in Fig. 21(a,b) depict the Grapheme-Al composite wear debris.

The dimensions of the debris were quantified, and it is apparent that the size of the wear debris ranged from submicron dimensions to over 100 microns. Furthermore at the interface between the test sample and the disk there is increase in temperature. During the progression of sliding, the fresh aluminum test sample undergoes exposure, rendering it active. However, as the sliding distance increases at elevated temperatures, the wear test reveals the occurrence of aluminum oxide formation at the interface. The results obtained from the Energy-Dispersive Spectroscopy (EDS) analysis provide confirmation that the formation of oxide occurs during the wear tests, the results are depicted in Fig. 21(b).

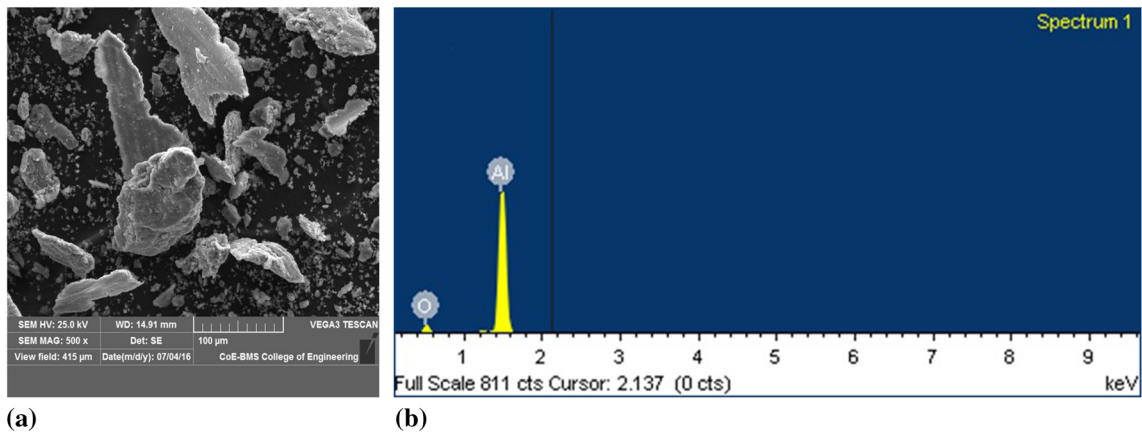


Fig. 20 (a) SEM of Pure Al wear debris. (b) EDS of Pure Al Debris

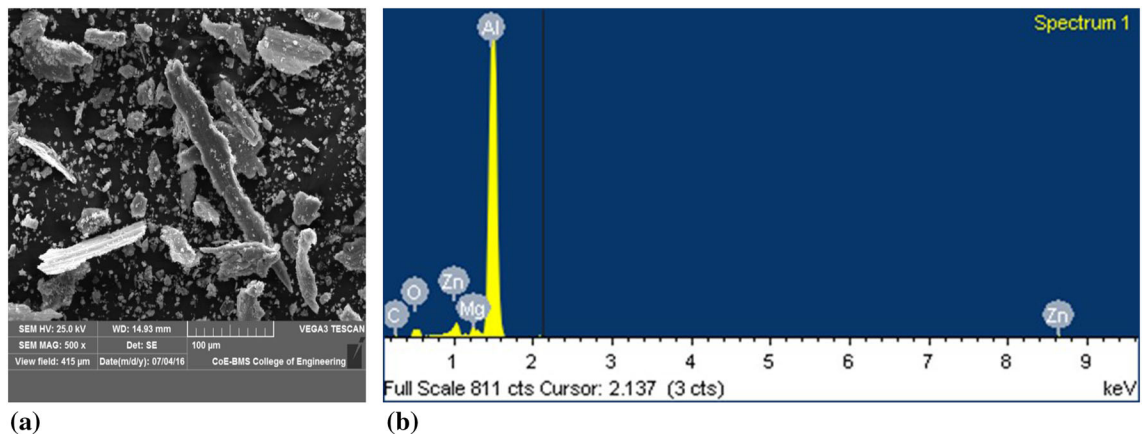


Fig. 21 (a) SEM of Composite wear debris. (b) EDS of Composite wear Debris

4. Conclusions

In this research, the influence of graphene reinforcement on aluminum matrix composites was synthesized, experimental tests were conducted to determine the wear behavior of the developed composites. The findings from the experimental tests are summarized as follows:

- SEM images confirm that the graphene particles are uniformly distributed in the aluminum matrix.
- Results of the optical microstructure reveal graphene dispersed homogeneously in aluminum. Grain size analysis confirmed that the graphene addition reduced the grain size of the Al-graphene composite when compared to the monolithic aluminum alloy.
- Addition of graphene (1 wt.%) to the aluminum matrix reduced both wear loss and the coefficient of friction.
- The wear rate of Al-Graphene composites is observed to be less compared to monolithic aluminum samples. Wear rate increases with the increase in velocity of sliding and load applied. The coefficient of friction of composite samples was less than that of pure aluminum samples. Al-Graphene composites exhibit superior tribological properties during tribological tests and exhibit a 38.1% reduction in wear rate at a load of 60 N.

References

1. M. Tabandeh-Khorshid, E. Omrani, P.L. Menezes and P.K. Rohatgi, Tribological Performance of Self-Lubricating Aluminum Matrix Nanocomposites: Role of Graphene Nanoplatelets, *Eng. Sci. Technol. Int. J.*, 2016, **19**(1), p 463–469
2. R. Derakhshandeh Haghighi, S.A. Jenabali Jahromi, A. Moresedgh and M. Tabandeh Khorshid, A Comparison Between ECAP and Conventional Extrusion for Consolidation of Aluminum Metal Matrix Composite, *J. Mater. Eng. Perf.*, 2012, **21**(9), p 1885–1892
3. M. Tabandeh Khorshid, S.A. Jenabali Jahromi and M.M. Moshksar, Mechanical Properties of Tri-modal Al Matrix Composites Reinforced by Nano- and Submicron-Sized Al_2O_3 Particulates Developed by Wet Attrition Milling and Hot Extrusion, *Mater. Des.*, 2010, **31**(8), p 3880–3884
4. Z.S. Toor and M.M. Zafar, Corrosion Degradation of Aluminium Alloys Using a Computational Framework, *Tribol. Mater.*, 2022, **1**(4), p 150–156
5. Z.S. Toor, Effect of Drill on Mechanical and Modal Characteristics of Aluminum Sheet, *J. Space Technol.*, 2021, **11**, p 14–19
6. B. Bobić, A. Vencl, M. Babić, S. Mitrović and I. Bobić, The Influence of Corrosion on the Microstructure of Thermally Treated ZA27/SiCp Composites, *Tribol. Ind.*, 2014, **36**(1), p 33–39
7. N. Idusuyi and J.I. Olayinka, Dry Sliding Wear Characteristics of Aluminium Metal Matrix Composites: A Brief Overview, *J. Mater. Res. Technol.*, 2019, **8**(3), p 3338–3346
8. C. Donnet and A. Erdemir, Historical Developments and New Trends in Tribological and Solid Lubricant Coatings, *Surf. Coat. Technol.*, 2004, **180–181**, p 76–84
9. C. Donnet and A. Erdemir, Solid Lubricant Coatings: Recent Developments and Future Trends, *Tribol. Lett.*, 2004, **17**(3), p 389–397

10. A. Vencl, I. Bobic and B. Stojanovic, Tribological Properties of A356 Al-Si Alloy Composites Under Dry Sliding Conditions, *Ind. Lubric. Tribol.*, 2014, **66**(1), p 66–74. <https://doi.org/10.1108/ILT-06-2011-0047>
11. P.K. Rohatgi, M. Tabandeh-Khorshid, E. Omrani, M.R. Lovell and P.L. Menezes, *Tribology of Metal Matrix Composites, Tribology for Scientists and Engineers*, Springer, New York, 2013, p 233–268
12. A. Revathi, S. Magesh, V.K. Balla, M. Das and G. Manivasagam, Current Advances in Enhancement of Wear and Corrosion Resistance of Titanium Alloys—A Review, *Mater. Technol.*, 2016, **31**(12), p 696–704
13. A. Moghadam, E. Omrani, P.L. Menezes and P.K. Rohatgi, Mechanical and Tribological Properties of Self-Lubricating Metal Matrix Nanocomposites Reinforced by Carbon Nanotubes (CNTs) and Graphene—A Review, *Compos. Part B Eng.*, 2015, **77**, p 402–420
14. B. Stojanović, S. Gajević, N. Kostić, S. Miladinović and A. Vencl, Optimization of Parameters that Affect Wear of A356/Al₂O₃ Nanocomposites Using RSM, ANN, GA and PSO Methods, *Ind. Lubric. Tribol.*, 2022, **74**(3), p 350–359. <https://doi.org/10.1108/ILT-07-2021-0262>
15. A. Vencl, F. Vučetić, B. Bobić et al., Tribological Characterisation in dry Sliding Conditions of Compcasted Hybrid A356/SiC_p/Gr_p Composites with Graphite Macroparticles, *Int. J. Adv. Manuf. Technol.*, 2019, **100**, p 2135–2146. <https://doi.org/10.1007/s00170-018-2866-0>
16. S. Zhang and X. Han, Effect of Different Surface Modified Nanoparticles on Viscosity of Nanofluids, *Adv. Mech. Eng.*, 2018, **10**(2), p 1687814018762011. <https://doi.org/10.1177/1687814018762011>
17. G. Bognár and A. Vencl, Experimental Investigation of Viscosity of Glycerol Based Nanofluids Containing Carbon Nanotubes, *Tribology in Industry*, 2019, **41**(2), p 267–273. <https://doi.org/10.24874/ti.2019.41.02.12>
18. S. Mosleh-Shirazi, F. Akhlaghi and L. Dong-yang, Effect of SiC Content on Dry Sliding Wear, Corrosion and Corrosive Wear of Al/SiC Nanocomposites, *Trans. Nonferr. Metals Soc. China*, 2016, **26**(7), p 1801–1808
19. G.M. Lin, G.Y. Xie, G.X. Sui and R. Yang, Hybrid Effect of Nanoparticles with Carbon Fibers on the Mechanical and Wear Properties of Polymer Composites, *Compos. Part B: Eng.*, 2012, **43**(1), p 44–49
20. D. Li, W. Yang, Y. Chen, C. Xiao and M. Wei, Effect of Modified Graphene on Thermal, Mechanical and Tribological Performance of Polyimide Based Composites, *Mater. Res. Express*, 2018, **5**(6), p 065304
21. X. Zeng, J. Yu, D. Fu, H. Zhang and J. Teng, Wear Characteristics of Hybrid Aluminum- Matrix Composites Reinforced with Well-Dispersed Reduced Graphene Oxide Nanosheets and Silicon Carbide particulates, *Vacuum*, 2018, **155**, p 364–375
22. B. Hekner, J. Myalski, N. Valle, A. Botor-Probierz, M. Sopicka-Lizer and J. Wiczorek, Friction and Wear Behavior of Al-SiC (n) Hybrid Composites with Carbon Addition, *Compos. Part B: Eng.*, 2017, **108**, p 291–300
23. H.T. Shivaramu and K.S. Umashankar, Dry Sliding Wear Behaviour of Multi Walled Carbon Nanotubes Reinforced Aluminium Composites Produced by Powder Metallurgy Technique, *Mater. Res. Express*, 2019, **6**(11), p 1150d7
24. J. Parmar, S.K. Patel, V. Katkar and A. Natesan, Graphene-Based Refractive Index Sensor Using Machine Learning for Detection of Mycobacterium Tuberculosis Bacteria, *IEEE Trans. Nanobiosci.*, 2023, **22**(1), p 92–98
25. S. Li, N. Liu, M. Becton, X. Zeng and X. Wang, Mechanics Prediction of 2D Architected Cellular Structures Using Transfer Learning, *J. Micromech. Mol. Phys.*, 2023, **8**(01), p 33–43
26. S.K.S. Hossain, S.S. Ali, S. Rushd, B.V. Ayodele and C.K. Cheng, Interaction Effect of Process Parameters and Pd-Electrocatalyst in Formic Acid Electro-Oxidation for Fuel Cell Applications: Implementing Supervised Machine Learning Algorithms, *Int. J. Energy Res.*, 2022, **46**(15), p 21583–21597
27. A. Vencl, Tribological Behavior of Ferrous-Based APS Coatings Under Dry Sliding Conditions, *J Therm Spray Tech*, 2015, **24**, p 671–682. <https://doi.org/10.1007/s11666-014-0202-2>
28. M.V. Nikolaos, V. Aleksandar, A. Emilija, K. Mara and P. Pandora, Scientific Literature on Thermal Spray Coatings from Southeastern Europe: A Ten Years Bibliometric Analysis, *FME Trans.*, 2019, **47**(3), p 649–657
29. M. Chandrasekaran, A.W. Batchelor and S. Jana, Friction Surfacing of Metal Coatings on Steel and Aluminum Substrate, *J. Mater. Process. Technol.*, 1997, **72**(3), p 446–452. [https://doi.org/10.1016/S0924-0136\(97\)00209-4](https://doi.org/10.1016/S0924-0136(97)00209-4)
30. Z. Hu, F. Chen, J. Xu, Q. Nian, D. Lin, C. Chen et al., 3D Printing Graphene-Aluminum Nanocomposites, *J. Alloy. Compd.*, 2018, **746**, p 269–276. <https://doi.org/10.1016/j.jallcom.2018.02.272SearchinGoogleScholar>
31. H. Asgharzadeh and M. Sedigh, Synthesis and Mechanical Properties of Al Matrix Composites Reinforced with Few-Layer Graphene and Graphene Oxide, *J. Alloy. Compd.*, 2017, **728**, p 47–62
32. J. Zhang, Z. Chen, J. Zhao and Z. Jiang, Microstructure and Mechanical Properties of Aluminium-Graphene Composite Powders Produced by Mechanical Milling, *Mech. Adv. Mater. Modern Process.*, 2018 <https://doi.org/10.1186/s40759-018-0037-5>
33. S.F. Bartolucci, J. Paras, M.A. Rafiee, J. Rafiee, S. Lee, D. Kapoor and N. Koratkar, Graphene-Aluminum Nanocomposites, *Mater. Sci. Eng. A*, 2011, **528**(27), p 7933–7937
34. M. Bastwros, G.-Y. Kim, C. Zhu, K. Zhang, S. Wang, X. Tang and X. Wang, Effect of Ball Milling on Graphene Reinforced Al6061 Composite Fabricated by Semi-Solid Sintering, *Compos. Part B*, 2014, **60**, p 111–118
35. L.-Y. Chen, H. Konishi, A. Fehrenbacher, C. Ma, J.-Q. Xu, H. Choi et al., Novel Nanoprocessing Route for Bulk Graphene Nanoplatelets Reinforced Metal Matrix Nanocomposites, *Script. Mater.*, 2012, **67**(1), p 29–32
36. K. Rajkumar and S. Aravindan, Tribological Behavior of Microwave Processed Copper-Nanographite Composites, *Tribol. Int.*, 2013, **57**, p 282–296
37. J. Wang, Z. Li, G. Fan, H. Pan, Z. Chen and D. Zhang, Reinforcement with Graphene Nanosheets in Aluminum Matrix Composites, *Script. Mater.*, 2012, **66**(8), p 594–597
38. S.J. Niteesh Kumar, R. Keshavamurthy, M.R. Haseebuddin et al., Mechanical Properties of Aluminium-Graphene Composite Synthesized by Powder Metallurgy and Hot Extrusion, *Trans Indian Inst Met*, 2017, **70**, p 605–613. <https://doi.org/10.1007/s12666-017-1070-5>
39. B.N. Yuyuths Gowda, M.R. Haseebuddin, B. Pal and R. Keshavamurthy, Mechanical and Wear Behaviour of Graphite Nano Filler Reinforced Al 6061 Composites, *Mater. Today: Proc.*, 2021, **46**, p 4504–4509. <https://doi.org/10.1016/j.matpr.2020.09.690>
40. M. Faraz, M.R. Haseebuddin and B. Pal, Mechanical Properties of Aluminium Metal Matrix Composite Reinforced with Silicon Carbide Using FEM, *IOP Conf. Series: Mater. Sci. Eng.*, 2021, **1013**(1), p 012013. <https://doi.org/10.1088/1757-899X/1013/1/012013>
41. R. Keshavamurthy, B.E. Naveena, C.S. Ramesh et al., Evaluation of Slurry Erosive Wear Performance of Plasma-Sprayed Flyash-TiO₂ Nanocomposite Coatings, *J Bio Tribo Corros*, 2021, **7**, p 92. <https://doi.org/10.1007/s40735-021-00525-4>
42. S. Basavaraja et al., Dry Sliding Wear Behaviour of Hybrid MMCs. ISSN 1392-1320, Vol No.3 (2015)
43. H. Deng, Z. Wang, X. Wang, R. Yang, H. Li, Z. Wang and X. Zhang, Graphene: A New Emerging Lubricant, *Mater. Today*, 2016, **19**(9), p 465–468
44. J. Li, Y. Zhang, M. Zhai, H. Jia, J. Wang, Y. Zheng and X. Qu, Friction and Wear Behavior of Aluminum Matrix Composites Reinforced with Graphene Nanoplatelets, *Wear*, 2013, **308**(1–2), p 32–37
45. M. Asif, M.W. Ashraf, S. Ahmad, U. Yaqoob and J. Luo, Role of Graphene in Friction and Wear, *AIP Adv.*, 2020, **10**(1), p 015228
46. Y. Wang, L. Chen, Z. Chen, S. Lin and X. Li, Graphene as a New Lubricating Additive in Oil, *Tribol. Int.*, 2014, **76**, p 191–197
47. T. Qiu, J. Wu, J. Xu, X. Sun and L. Yu, Mechanisms of Friction Reduction by Graphene Coatings, *Carbon*, 2013, **55**, p 173–178
48. X. Zhang, H. Guo, X. Cao, Z. Tang, Y. Zhu, J. Huang and L. Jiang, Enhanced Wear Resistance of Graphene/Aluminum Composites Prepared by Spark Plasma Sintering, *Carbon*, 2015, **94**, p 462–470
49. Y. Hu, X. Zeng, J. Zhao, S. Du, B. Liu, C. Chen and L. Li, Graphene Nanoplatelets/Aluminum Composites: Wear Behavior and Mechanisms, *J. Mater. Sci.*, 2017, **52**(5), p 2511–2524
50. J. Li, H. Zhang, G. Du, X. Jiang, Y. Cheng and X. Shen, Enhanced Wear Resistance and Friction Properties of Aluminum Composites Reinforced with Graphene Nanoplatelets, *J. Mater. Sci. Technol.*, 2019, **35**(5), p 888–897

51. S.C. Lim, Y.F. Ho, M.S. Bharathi and M.M. Rahman, Graphene-Reinforced Aluminum as a Nanocomposite Solid Lubricant, *Tribol. Lett.*, 2016, **63**(1), p 1–9

Publisher's Note Springer Nature remains neutral with regard to jurisdictional claims in published maps and institutional affiliations.

Springer Nature or its licensor (e.g. a society or other partner) holds exclusive rights to this article under a publishing agreement with the author(s) or other rightsholder(s); author self-archiving of the accepted manuscript version of this article is solely governed by the terms of such publishing agreement and applicable law.